

Synthesis and Structures of Highly Conducting Charge-Transfer Salts of Selenium Containing TTM-TTP Derivatives

Minoru Ashizawa, Akane Akutsu, Bunpei Noda, Hirofumi Nii, Tadashi Kawamoto, Takehiko Mori,* Takashi Nakayashiki,[1] Yohji Misaki,[1] Kazuyoshi Tanaka,[1] Kazuo Takimiya,[2] and Tetsuo Otsubo[2]

Department of Organic and Polymeric Materials, Graduate School of Science and Engineering, Tokyo Institute of Technology, O-okayama, Meguro-ku, Tokyo 152-8552

[1]Department of Molecular Engineering, Graduate School of Engineering, Kyoto University, Katsura, Kyoto 615-8510

[2]Department of Applied Chemistry, Graduate School of Engineering, Hiroshima University, Higashi-Hiroshima 739-8527

Received January 26, 2004; E-mail: takehiko@o.cc.titech.ac.jp

Selenium-substituted TTM-TTP (2,5-bis[4,5-bis(methylthio)-1,3-dithiol-2-ylidene]-1,3,4,6-tetrathiapentalene) derivatives (**1a**–**1d**), in which several 1,3-dithiole rings of the bis-fused TTF framework are replaced by 1,3-diselenole rings, have been prepared. In particular, we have accomplished the first selenium substitution of the inner TTP part (**1a**). The 1:1 composition iodine salt, (**1a**)I_3, is an insulator constructed of the donor trimers. The 1:1 $GaCl_4$ salt, (**1a**)$GaCl_4$, has a uniform column isostructural to the sulfur analog, (TTM-TTP)$FeBr_{1.8}Cl_{2.2}$; it exhibits metallic conduction down to about 60 K, the lowest metal–insulator (M–I) transition temperature in 1:1 salts. The donors **1c** and **1d** give the iodine salts isostructural to the sulfur analog, (TTM-TTP)$(I_3)_{5/3}$. By the selenium substitution, the M–I transition of (**1d**)$(I_3)_{5/3}$ is entirely suppressed.

Tetrathiafulvalene (TTF)[1] and its derivatives have been extensively investigated as components of organic conductors and superconductors.[2] Earlier investigations of (TTF)(TCNQ) (TCNQ: tetracyanoquinodimethane) and other TTF complexes have revealed that TTF complexes are one-dimensional conductors and are susceptible to the Peiels transition.[3] It was soon found, however, that the substitution of the sulfur atoms with selenium atoms, namely TSF (tetraselenafulvalene), greatly enhances the interchain interactions to stabilize the metallic state.[4] Along this line, the first organic superconductors based on TMTSF (tetramethyltetraselenafulvalene) have been prepared.[5] Nonetheless only a limited number of TSF derivatives have been prepared owing to the synthetic difficulty; it is sometimes necessary to use such hazardous starting materials as CSe_2 and H_2Se, though several improved methods that do not use these materials have been reported.[6] Recently, however, Ogura and Takimiya have reported an improved synthesis of CSe_2.[7] Based on this material, together with a new synthetic route starting from trimethylsilylacetylenes, a facile synthesis of 1,3-diselenole-2-selenone has been established,[8] and a large number of TSF derivatives have been prepared.[9]

On the other hand, as an attempt to explore new π-electron systems derived from TTF, bis-fused TTF derivatives (TTP: tetrathiapentalenes), have been developed. These TTP donors have produced a large number of metallic cation-radical salts.[10] In particular, TTM-TTP (2,5-bis[4,5-bis(methylthio)-1,3-dithiol-2-ylidene]-1,3,4,6-tetrathiapentalene)[11] (Scheme 1) has formed several attractive salts, including metallic organic conductors having 1:1 composition, (TTM-TTP)I_3,[12] (TTM-TTP)$[C(CN)_3]$,[13] (TTM-TTP)$FeBr_{1.8}Cl_{2.2}$,[14] and (TTM-TTP)$Fe_{0.9}Ga_{0.1}Cl_4$.[15] Although other 1:1 organic metals, (DMTSA)BF_4 (DMTSA = 2,3-dimethyltetraselenoanthracene)[16] and (BETS)$GaBr_4$ (BETS = bis(ethylenedithio)tetraselenafulvalene),[17] have been reported, the TTM-TTP salts provide the most rich variety of 1:1 organic metals. In addition, TTM-TTP forms a charge-transfer salt with a high oxidation state exceeding +1, (TTM-TTP)$(I_3)_{5/3}$.[18] Although most of the highly conducting TTF salts are quarter-filled with +1/2 donor charges, (TTM-TTP)$(I_3)_{5/3}$ has a large donor charge of +5/3, but shows metallic conduction down to about 20 K. These TTP salts have uniform donor columns irrespective of counter anions, and are highly one-dimensional. Since the Coulomb interaction is of essential importance in localizing the conducting electrons, a one-dimensional system is more susceptible to electron correlation than a two-dimensional system. Therefore a one-dimensional system is usually associated with a transition to an insulating ground state.

In order to improve the conducting properties, we have chosen TTM-TTP as an example to explore the synthetic methods for the selenium substitution. We have already reported TSM-TTP (2,5-bis[4,5-bis(methylseleno)-1,3-dithiol-2-ylidene]-1,3,4,6-tetrathiapentalene), a selenium analog of TTM-TTP, in which the terminal methylthio groups are replaced by methylseleno groups.[19] TSM-TTP gives a metallic salt, (TSM-TTP)$(I_3)_{5/3}$, that is isostructural to the sulfur analog, (TTM-TTP)$(I_3)_{5/3}$. In addition, several selenium containing TTP-type donors including the vinylogous DTEDT (2-(1,3-dithiol-2-ylidene)-5-(2-ethanediylidene-1,3-dithiole)-1,3,4,6-tet-

Published on the web August 6, 2004; DOI 10.1246/bcsj.77.1449

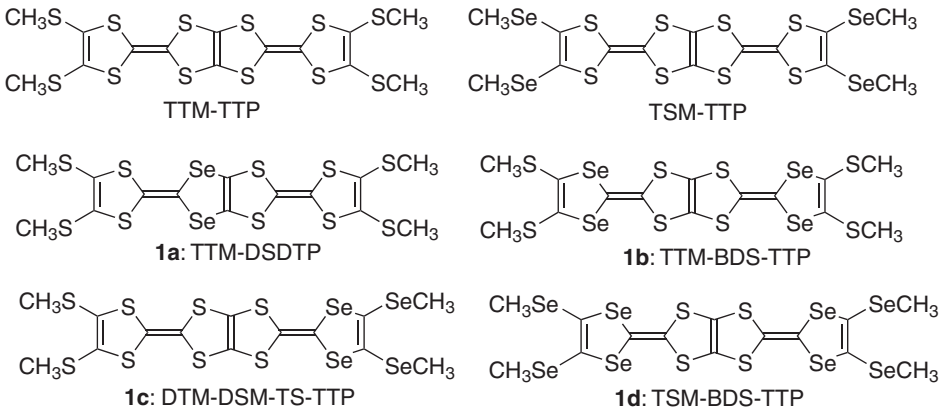

Scheme 1. TTM-TTP type organic donors.

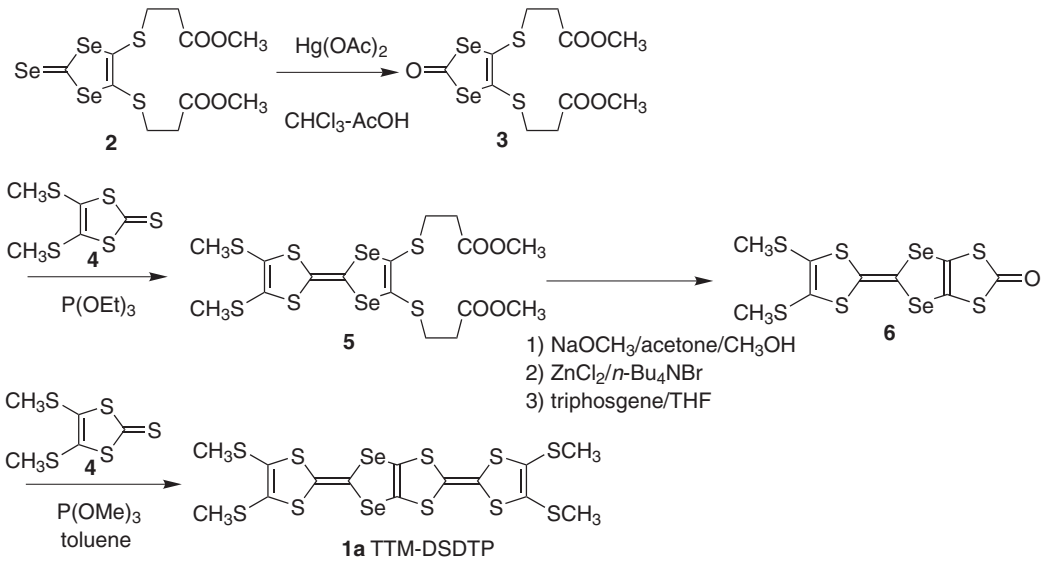

Scheme 2. Synthesis of TTM-DSDTP (**1a**).

rathiapentalene), in which the outer 1,3-dithiole rings of the bis-fused TTF framework are replaced by 1,3-diselenole rings, have been developed.[20,21]

From the viewpoint of synthetic chemistry, the synthesis of selenium containing TTP donors has not been well explored. In particular, the selenium substitution of the central TTP core has not been accomplished. In the present paper, we report the syntheses of the selenium containing TTM-TTP derivatives **1a**–**1d**. In TTM-DSDTP (2,5-bis[4,5-bis(methylthio)-1,3-dithiol-2-ylidene]-1,3-diselena-4,6-dithiapentalene: **1a**), two sulfur atoms of the inner TTP unit are substituted by selenium. Both of the two outer 1,3-dithiole rings are replaced by 1,3-diselenole rings, where the terminal parts remain SCH_3 in TTM-BDS-TTP (2,5-bis[4,5-bis(methylthio)-1,3-diselenol-2-ylidene]-1,3,4,6-tetrathiapentalene: **1b**), whereas those are replaced by $SeCH_3$ in TSM-BDS-TTP (2,5-bis[4,5-bis(methylseleno)-1,3-diselenol-2-ylidene]-1,3,4,6-tetrathiapentalene: **1d**). Only one of the outer 1,3-dithiole rings is replaced by selenium in DTM-DSM-TS-TTP (2-[4,5-bis(methylthio)-1,3-dithiol-2-ylidene]-5-[4,5-bis(methylseleno)-1,3-diselenol-2-ylidene]-1,3,4,6-tetrathiapentalene: **1c**). In addition, the structures and conducting properties of several salts of these new donors are described and compared with the TTM-TTP salts. Investigations of their conducting properties and band calculations based on the X-ray structure analyses demonstrate the merits of the selenium substitution.

Results and Discussion

Synthesis and Electrochemistry of Selenium-Containing TTM-TTP Derivatives. The synthesis of **1a** is outlined in Scheme 2. We used carbon diselenide as the starting material.[7] The compound **2**, 4,5-bis[2-(methoxycarbonyl)ethylthio]-1,3-diselenole-2-selone, was prepared according to the previous reports.[8,22] This compound was easily converted to the corresponding ketone **3** by using $Hg(OAc)_2$. The construction of the diselenadithiapentalene (DSDTP) framework was achieved by the two-step cross-coupling reactions.[11] Thione **4** and ketone **3** were cross-coupled in neat triethylphosphite at 110 °C to afford unsymmetrical diselenadithiafulvalene **5** in 96% yield. Compound **5** was allowed to react with excess sodium methoxide in acetone–methanol at room temperature, followed by treatment with anhydrous zinc chloride and tetrabutylammonium bromide, and then with an excess of triphosgene in THF at −78 °C to provide diselenadithiafulvalene-fused 1,3-dithiol-2-

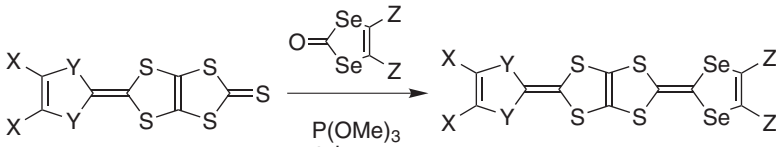

1b X = SCH_3, Y = Se, Z = SCH_3: TTM-BDS-TTP
1c X = SCH_3, Y = S, Z = $SeCH_3$: DTM-DSM-TS-TTP
1d X = $SeCH_3$, Y = Se, Z = $SeCH_3$: TSM-BDS-TTP

Scheme 3. Synthesis of TTM-BDS-TTP (**1b**), DTM-DSM-TS-TTP (**1c**), and TSM-BDS-TTP (**1d**).

Table 1. Redox Potentials/V[a)]

Compound	$E^1_{1/2}$	$E^2_{1/2}$	$E^3_{1/2}$	E^4_{ox}	$E_2 - E_1$
1a	0.40	0.63	0.86		
1b	0.46	0.68	0.93	1.21[b)]	0.22
1c	0.45	0.69	0.93	1.14[b)]	0.24
1d	0.53	0.74	0.93	1.16[b)]	0.21
TTM-TTP	0.48	0.67	0.89	1.01	0.19

a) vs Ag/AgCl in *n*-Bu_4NPF_6/benzonitrile at a Pt working electrode, 25 °C, scan rate 25, 50, and 100 mV s^{-1}. The listed values are averages for the three scan rates. As a reference, the redox potential of ferrocene is 0.46 V under identical conditions. b) The oxidation peaks are shown on account of the irreversibility, except for $E^4_{1/2}$ for TTM-TTP.

Table 2. Electrical Properties of Charge-Transfer Salts of DA_x

Donor	Anion (A)	Form	x	σ_{rt}/S cm^{-1}	E_a/eV
TTM-DSDTP (**1a**)	AsF_6	black needle	0.5[a)]	0.3	0.15
	PF_6	black needle	0.56[a)]	3.6	0.04
	I_3	black needle	1[b)]	2.3	0.11
	$GaCl_4$	black block	1[b)]	280	metallic, $T_{MI} = 60$ K
DTM-DSM-TS-TTP (**1c**)	I_3	copper plate	5/3[c)]	520	metallic, $T_{MI} = 25$ K
TSM-BDS-TTP (**1d**)	I_3	copper plate	5/3[c)]	630	metallic down to 4.2 K

a) Determined based on measurements of energy dispersion spectroscopy (EDS), the compositions of the **1a**, to the anions of AsF_6 and PF_6 are determined by energy dispersion spectroscopy (EDS) from the ratio of S and As for the AsF_6 salt, and S and P for the PF_6 salt. b) Determined from the X-ray single crystal analysis. c) Determined from the X-ray single crystal analysis and X-ray oscillation photograph.

one **6** (47% yield). By a cross-coupling reaction of compounds **6** and **4** with a large excess of trimethylphosphite in refluxing toluene, the target molecule TTM-DSDTP (**1a**) was obtained as a brown solid in 38% yield. Other compounds **1b**–**1d** were prepared similarly (Scheme 3).[23]

The solution redox properties of newly prepared TTM-TTP derivatives have been studied by cyclic voltammetry. The results are listed in Table 1. The compounds **1b**–**1d** show three pairs of reversible redox waves and an irreversible one up to tetra cations, which correspond to the stepwise oxidation of the four 1,3-dithiole rings. The first redox potential of **1d**, in which the sulfur atoms in the outer 1,3-dithiole rings together with the terminal methylthio groups are replaced by selenium atoms, is 0.05 V higher than that of TTM-TTP. This tendency has been observed in the selenium containing TMET-TTP derivatives.[23] In contrast, the redox behavior of TTM-DSDTP (**1a**) is somewhat different and more complicated. Three redox waves are observed, and the fourth step is not clearly obtained, in comparison with other donors. The first redox potential of **1a** is 0.08 V lower than that of TTM-TTP. In general, the selenium substitution of the 1,3-dithiole rings (e.g., TTF → TSF) weakens the donor ability. The observed shift of **1a** is opposite to this general rule. The substitution of $-SCH_3$ to $-SeCH_3$, however, increases the donor ability. The observed shift seems as if the first oxidation occurred mainly on the outer rings, so that the Se substitution to the inner rings worked like the $-SeCH_3$ substitution.

Charge-transfer salts of the present donors have been prepared by electrochemical oxidation in the presence of tetrabutylammonium salts of various anions. The obtained salts are listed in Table 2. TTM-DSDTP (**1a**) forms complexes with AsF_6^-, PF_6^-, I_3^-, and $GaCl_4^-$. The AsF_6^- and PF_6^- salts have a 2:1 composition, as determined from energy dispersion spectroscopy (EDS). The I_3^- and $GaCl_4^-$ salts are 1:1 salts as revealed by X-ray structure analyses. On the contrary, we have obtained the (TTM-TTP)$(I_3)_{5/3}$-type salts for DTM-DSM-TS-TTP (**1c**) and TSM-BDS-TTP (**1d**). Unfortunately, the charge-transfer salts of TTM-BDS-TTP (**1b**) have not been obtained, yet.

Crystal Structures of (1a)I_3 and (1a)$GaCl_4$. (1a)I_3: The crystallographic data are listed in Table 3. This salt has a 1:1 composition, but is not isostructural with the sulfur analog, (TTM-TTP)I_3. The molecular structure of the donor molecule is shown in Figs. 1(a) and 1(b). The one and half donor molecules are crystallographically independent; the molecule A is

Table 3. Crystallographic Data of (**1a**)I_3 and (**1a**)$GaCl_4$ Together with (TTM-TTP)$FeBr_{1.8}Cl_{2.2}$

	(**1a**)I_3	(**1a**)$GaCl_4$	(TTM-TTP)$FeBr_{1.8}Cl_{2.2}$
Chemical formula	$C_{21}H_{18}S_{15}Se_3I_{4.5}$	$C_{14}H_{12}S_{10}Se_2GaCl_4$	$C_{14}H_{12}S_{12}FeBr_{1.8}Cl_{2.2}$
Formula weight	1559.22	870.30	842.64
Shape	Black needle	Black block	Black block
Crystal system	Triclinic	Monoclinic	Monoclinic
Space group	$P\bar{1}$	$C2/c$	$C2/c$
a/Å	9.9035(8)	24.065(7)	23.975(5)
b/Å	13.871(2)	5.922(2)	5.874(1)
c/Å	15.586(2)	22.441(5)	22.772(4)
α/°	98.449(4)		
β/°	91.074(2)	118.58(2)	118.24(1)
γ/°	105.0833(13)		
V/Å^3	2041.2(4)	2808(1)	2825(1)
Z	2	4	4
D_{calcd}/g cm^{-3}	2.537	2.058	2.002
μ/mm^{-1}	6.895	4.703	2.227
Temperature	r.t.	r.t.	r.t.
Reflections measured	8849	4473	4609
Reflections used	4847 ($I > 3\sigma(I)$)	1318 ($I > 3\sigma(I)$)	2207 ($I > 4\sigma(I)$)
$R^{a)}/R_w^{b)}$	0.057/0.062	0.051/0.056	0.034/0034

a) $R = \Sigma||F_o| - |F_c||/\Sigma|F_o|$. b) $R_w = [\Sigma w(|F_o| - |F_c|)^2/\Sigma wF_o^2]^{1/2}$.

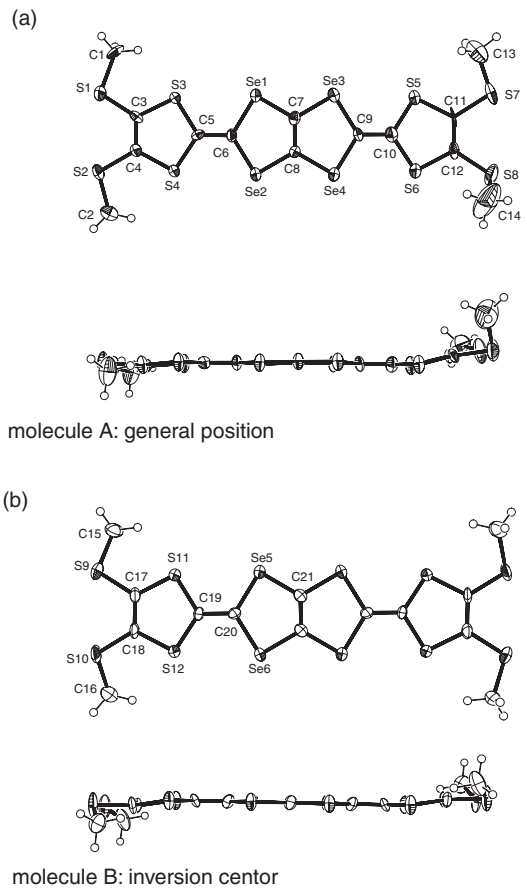

Fig. 1. ORTEP drawing and atomic numbering scheme of donors of (**1a**)I_3. (a) The molecule A located on a general position and (b) the molecule B located on an inversion center.

located on a general position, whereas the molecule B exists on an inversion center. The anions exist as isolated I_3^-, and one and half anions are crystallographically independent similarly to the donor part. Then one unit cell contains three donors and three isolated I_3^- anions, and the composition is exactly 1:1. The molecule A is almost flat, but slightly bents at one of the outer 1,3-dithiole rings. The terminal methyl groups are located in the molecular plane except for one methyl group that extends out of the molecular plane. On the other hand, the donor B is almost planar, though the terminal methyl groups slightly deviate from the molecular plane. The selenium atoms in the central TTP core of the molecules A and B are treated as disordered. This disorder in the molecules A and B is confirmed by the population analysis that assumes the selenium occupancy of 0.5 within the experimental error. Figure 2 shows the crystal structure and the overlap mode of (**1a**)I_3. The donors make a trimer A–B–A; the interplanar distance is 3.47 Å and the donors slip along the molecular long axis (1.86 Å).

Although the intramolecular bond lengths of the present salt are not accurate enough to give conclusive information about the charge transfer, if we compare the bond lengths of all C=C bonds of molecules A and B, the C=C bond lengths of molecule A are slightly shorter than those of molecule B.[12,24] This implies that molecule A has a smaller positive charge than molecule B, and that the central B molecule has to have a charge somewhat exceeding 1+.

(1a)$GaCl_4$: Crystallographic data are listed in Table 3. This compound is isostructural to the 1:1 composition salt, (TTM-TTP)$FeBr_{1.8}Cl_{2.2}$,[14] though all lattice constants of the present selenium salt are larger. Figures 3(a) and 3(b) show the molecular structure and the crystal structure. The donors are located on inversion centers, so that half of the donor is crystallographically independent, whereas a $GaCl_4^-$ anion is located on a 2-fold axis. The donor molecule is almost planar; one of the two independent terminal methyl groups (C_1 and C_2) extends out of the molecular plane and the other is located in the plane. This

resembles the 1+ donors in the same structure with the space group $C2/c$.[13,14] The donors form uniform stacks along the *b* axis. The interplanar distance between the donors is 3.44 Å and the slip distance along the molecular long axis is 4.82 Å. These values are almost the same as those of other TTM-TTP based organic metals with a 1:1 composition.[12]

Energy Band Structure of (1a)$GaCl_4$. The tight-binding band structure is calculated from the intermolecular overlap integrals of HOMO (Table 4); b is the intrastack interaction along the *b* axis, and p1–p3 show interstack interactions where three transverse interactions exist along the *c* axis (Fig. 3).[25] Such calculations are very useful in understanding the electronic structure of molecular conductors, but the treatment of the selenium-containing salts does not easily provide a complete picture of the electronic structure and requires much attention to that evaluation.[26] In the present calculation of HOMO, we have treated four chalcogen atoms of the central TTP core as selenium atoms because of the selenium disorder.[26] The ratio of the calculated intrastack b and interstack p overlap integrals is about 100:1, indicating high one-dimensionality. The resulting Fermi surface is open (Fig. 4). The b interaction along the stacking direction is, however, larger, and the bandwidth (1.2 eV) is broader than the values for (TTM-TTP)$FeBr_{1.8}Cl_{2.2}$ (0.8 eV). Because all disordered chalcogen atoms are treated as selenium, we have to take account of the resulting overestimation, but the obtained large intrastack interaction is regarded as the actual effect of the selenium substitution.[27]

Transport Properties of Charge-Transfer Salts of 1a. The room-temperature conductivities of the PF_6^- and AsF_6^- salts, 3.6 and 0.3 S cm^{-1}, are not so high (Table 2); both salts show semiconductive behavior, with the activation energies

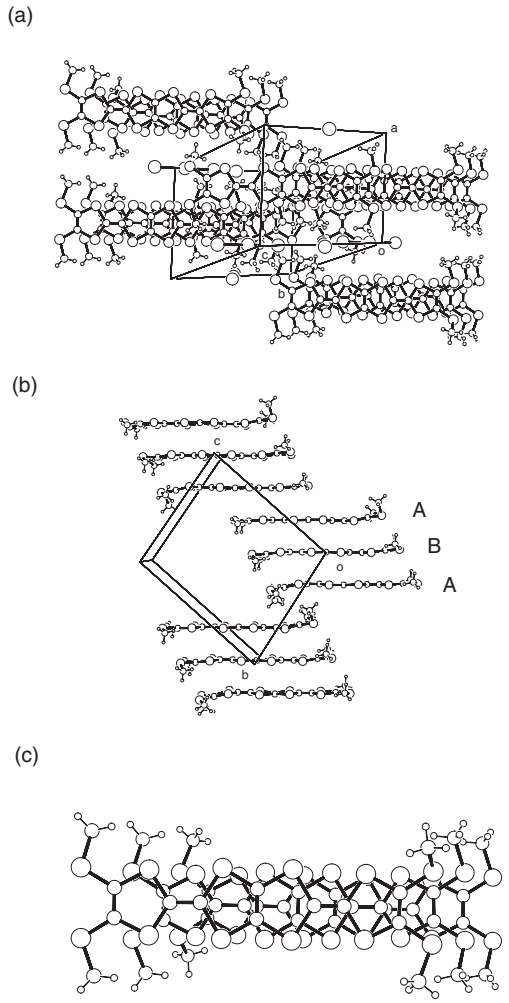

Fig. 2. Crystal structure of (**1a**)I_3. (a) Projected in the trimer stacking direction, (b) viewed along the molecular short axis, and (c) overlap mode of the donors.

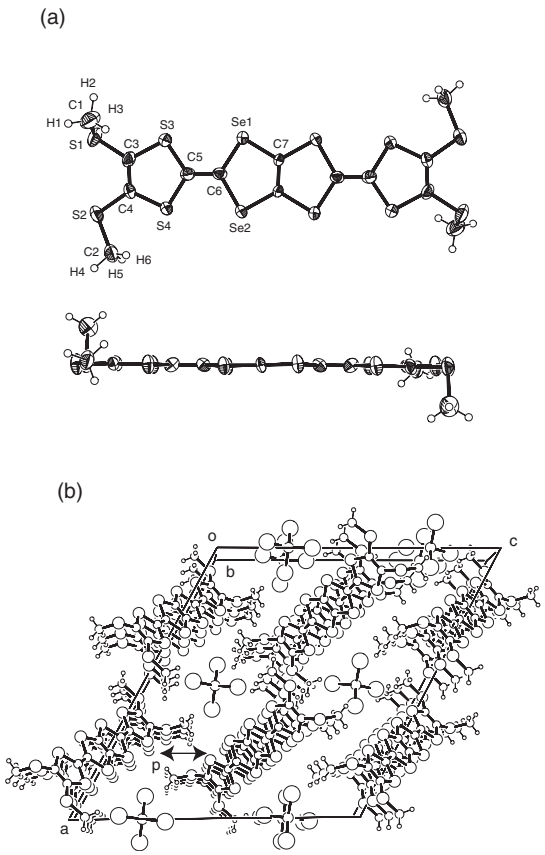

Fig. 3. Crystal structure of (**1a**)$GaCl_4$. (a) ORTEP drawing and atomic numbering scheme of the donor of (**1a**)$GaCl_4$ and (b) projection on the *ac* plane.

Table 4. The Intermolecular Overlap Integrals ($\times 10^{-3}$) of the Present Salt Together with (TTM-TTP)$FeBr_{1.8}Cl_{2.2}$[14]

	b	p1 [0, −1/2, 1/2][a)]	p2 [0, 1/2, 1/2][a)]	p3 [0, 3/2, 1/2][a)]
(**1a**)$GaCl_4$	−31.8	0.20	0.23	0.02
(TTM-TTP)$FeBr_{1.8}Cl_{2.2}$	−20.9	0.12	0.13	0.01

a) The brackets indicate the directions of p1–p3 interactions.

of 0.04 and 0.15 eV, respectively. (**1a**)I_3 also has a low conductivity of 2.3 S cm^{-1} at room temperature and is semiconductive with the activation energy of 0.11 eV. This is related to the trimer structure of the donors.

In contrast, (**1a**)$GaCl_4$ shows very high conductivity, about 280 S cm^{-1} at room temperature. In Fig. 5(a), the normalized resistivity is compared to (TTM-TTP)$FeBr_{1.8}Cl_{2.2}$, which shows the gradual stepwise increase of resistivity below 160 K. In contrast, (**1a**)$GaCl_4$ shows basically constant resistivity down to about 60 K, below which the resistivity exhibits a steep increase and the compound becomes an insulator. It is clear that the temperature showing the steep increase of resistivity is shifted to lower temperatures. In (TTM-TTP)I_3[12] and (TTM-TTP)$[C(CN)_3]$,[13] the M–I transitions, where the steep increase of resistivity is observed, are recorded at 160 K and 70 K, respectively. Among these salts, (**1a**)$GaCl_4$ has the lowest M–I transition temperature (60 K). This may be related to the large bandwidth realized by the selenium substitution.

The thermoelectric power of (**1a**)$GaCl_4$ takes a small negative value (−2.6 μV K^{-1} at room temperature) and is approximately constant from room temperature to about 100 K (Fig. 5(b)), below which the thermopower diverges. This resembles (TTM-TTP)$FeBr_{1.8}Cl_{2.2}$ and supports the existence of a half-filled band.[12]

Crystal Structures of (1c)$(I_3)_{5/3}$ and (1d)$(I_3)_{5/3}$. Crystallographic data of (**1c**)$(I_3)_{5/3}$ and (**1d**)$(I_3)_{5/3}$, in comparison with (TTM-TTP)$(I_3)_{5/3}$,[18] are listed in Table 5. The lattice constants are almost the same, indicating that these salts are isostructural. All lattice constants of the Se compounds increase as the selenium contents, namely as **1d** > **1c** > TTM-TTP.

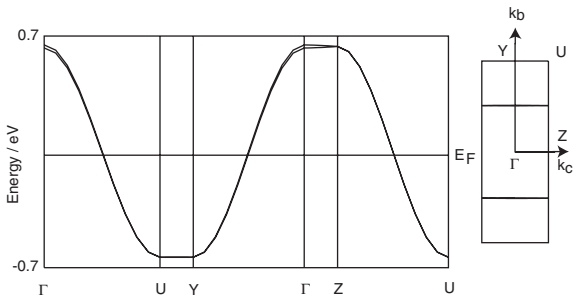

Fig. 4. Band structure and Fermi surface of (**1a**)$GaCl_4$.

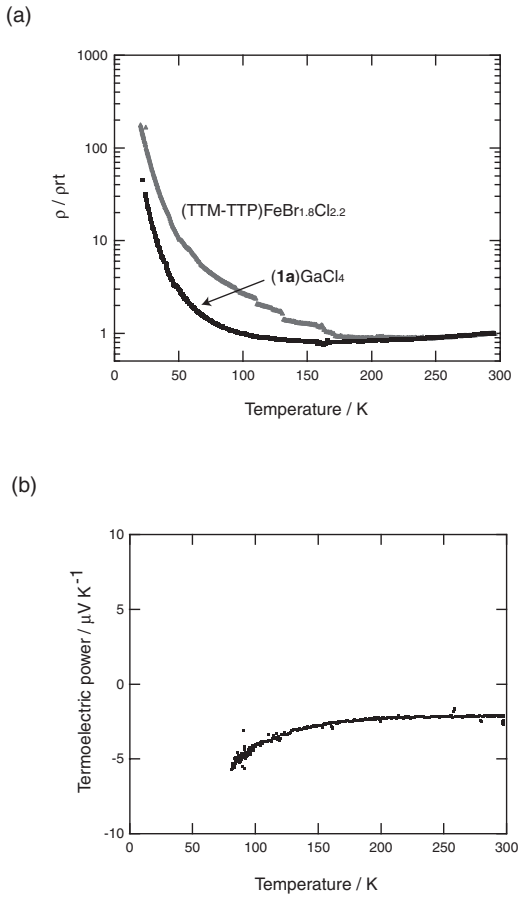

Fig. 5. Transport properties of (**1a**)$GaCl_4$. (a) Normalized electrical resistivity of (**1a**)$GaCl_4$ together with (TTM-TTP)$FeBr_{1.8}Cl_{2.2}$ and (b) thermoelectric power of (**1a**)$GaCl_4$.

Table 5. Crystallographic Data of (**1c**)$(I_3)_{5/3}$ and (**1d**)$(I_3)_{5/3}$ Together with (TTM-TTP)$(I_3)_{5/3}$[c)]

	(**1c**)$(I_3)_{5/3}$	(**1d**)$(I_3)_{5/3}$	(TTM-TTP)$(I_3)_{5/3}$
Chemical formula	$C_{14}H_{12}S_8Se_4I_5$	$C_{14}H_{12}S_4Se_8I_5$	$C_{14}H_{12}S_{12}I_5$
Formula weight	1387.09	1574.69	1199.49
Shape	Copper plate	Copper plate	Copper plate
Crystal system	Orthorhombic	Orthorhombic	Orthorhombic
Space group	*Cmmm*	*Cmmm*	*Cmmm*
a/Å	6.2774(8)	6.321(3)	6.247(4)
b/Å	18.959(2)	19.083(9)	18.68(2)
c/Å	12.991(2)	13.15(1)	12.804(7)
V/Å^3	1546.1(3)	1583(1)	1491(1)
Z	2	2	2
D_{calcd}/g cm^{-3}	2.979	3.304	2.666
μ/mm^{-1}	10.289	14.389	5.967
Temperature	r.t.	r.t.	r.t.
Reflections measured	1310	1337	1524
Reflections used	636 ($I > 3\sigma(I)$)	450 ($I > 5\sigma(I)$)	774 ($I > 5\sigma(I)$)
$R^{a)}/R_w^{b)}$	0.056/0.065	0.095/0.111	0.080/0.091

a) $R = \Sigma||F_o| - |F_c||/\Sigma|F_o|$. b) $R_w = [\Sigma w(|F_o| - |F_c|)^2/\Sigma wF_o^2]^{1/2}$. c) Ref. 18.

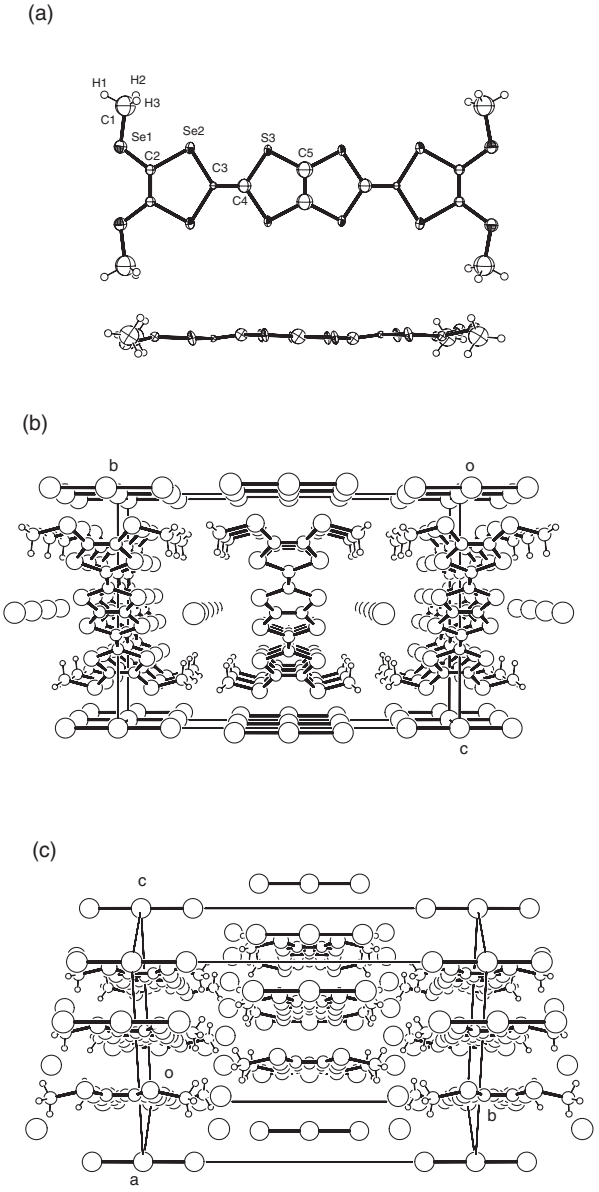

Fig. 6. Crystal structure of (**1c**)$(I_3)_{5/3}$. (a) ORTEP drawing and atomic numbering scheme of the donor of (**1c**)$(I_3)_{5/3}$, (b) projection along the *a* axis, and (c) view from the molecular long axis.

The molecular structure is shown in Fig. 6(a). The donor molecule is essentially planar and the terminal methyl groups extend in the molecular plane. As shown in Fig. 6(b), the donors form a uniform stack along the *a* axis. The interplanar distances of the neighboring donors in the stack are 3.43 Å for **1c** and 3.42 Å for **1d** (cf. 3.39 Å for TTM-TTP).

As to the anion parts, there are two kinds of anions (Figs. 6(b) and 6(c)). One is discrete I_3^-, which is located on the origin with *mmm* symmetry, and extends along the *b* axis. The other anion makes an infinite chain along the *a* axis. It is well known that iodine anions frequently form infinite chains, where the actual units which constitute the chain are I^-, I_3^-, or I_5^-.[28] In an average structure analysis such as the present analysis, however, an infinite chain with regular intervals is observed instead. The average iodine spacing, 3.14 Å for (**1c**)$(I_3)_{5/3}$ and 3.16 Å for (**1d**)$(I_3)_{5/3}$, is typical of infinite iodine chains. In the present case, the oscillation photographs of (**1c**)$(I_3)_{5/3}$ and (**1d**)$(I_3)_{5/3}$ show a few spots at $2a^*/3$. The repeating units $(3/2)a$ are 9.42 Å for (**1c**)$(I_3)_{5/3}$ and 9.48 Å for (**1d**)$(I_3)_{5/3}$. These values correspond to the typical length of the repeating unit of the I_3^- chain. Therefore, the anion part is composed of the discrete I_3^- and the infinite chain of I_3^-, both without any observable deficiency, so that the compositions are determined to be (**1c**)$(I_3)_{5/3}$ and (**1d**)$(I_3)_{5/3}$.

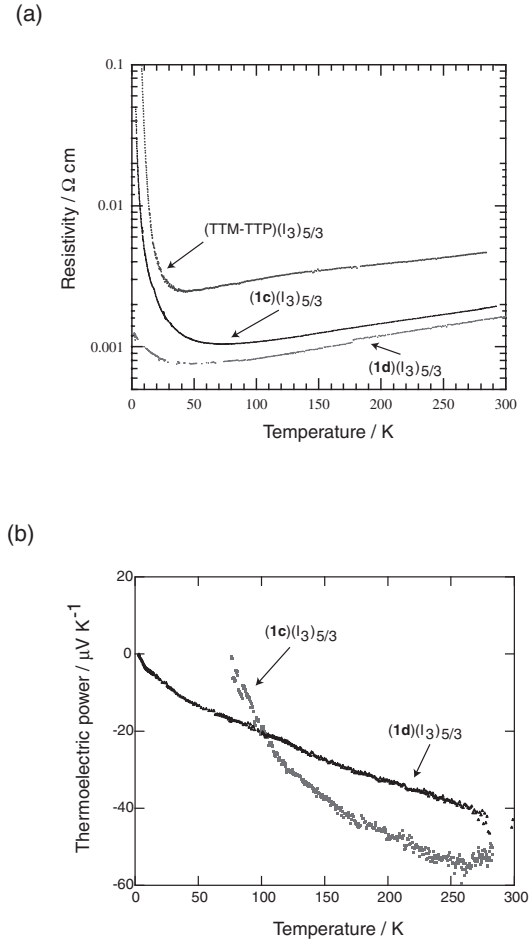

Fig. 7. Transport properties of the 5/3-phase salts. (a) Electrical resistivity of (**1c**)$(I_3)_{5/3}$, and (**1d**)$(I_3)_{5/3}$ together with (TTM-TTP)$(I_3)_{5/3}$ and (b) thermoelectric power of (**1c**)$(I_3)_{5/3}$, and (**1d**)$(I_3)_{5/3}$.

Transport Properties of (1c)$(I_3)_{5/3}$ and (1d)$(I_3)_{5/3}$. The temperature dependence of electrical resistivity of (**1c**)$(I_3)_{5/3}$ and (**1d**)$(I_3)_{5/3}$ is shown in Fig. 7(a). The room-temperature conductivities increase in the order of (TTM-TTP)$(I_3)_{5/3}$[18] (200 S cm^{-1}) < (**1c**)$(I_3)_{5/3}$ (520 S cm^{-1}) < (**1d**)$(I_3)_{5/3}$ (630 S cm^{-1}). The resistivity of (**1c**)$(I_3)_{5/3}$ shows a metallic decrease down to about 25 K, below which an M–I transition takes place. The positional disorder of selenium and sulfur atoms in the **1c** molecule may be responsible for this transition. In contrast, (**1d**)$(I_3)_{5/3}$ shows essentially constant resistivity down to liquid helium temperature. Compared with (TTM-TTP)$(I_3)_{5/3}$, the M–I transition is not suppressed in (**1c**)$(I_3)_{5/3}$, whereas in (**1d**)$(I_3)_{5/3}$ the transition is suppressed completely and the metallic phase is stabilized.

Table 6. The Intermolecular Overlap Integrals ($\times 10^{-3}$) of the Present Salts Together with (TTM-TTP)$(I_3)_{5/3}$[18]

	a	b	c
(**1c**)$(I_3)_{5/3}$ (Se)[a)]	20.3	0.08	8.3
(**1c**)$(I_3)_{5/3}$ (S)[a)]	14.1	0.05	2.5
(**1d**)$(I_3)_{5/3}$	13.7	0.16	9.2
(TTM-TTP)$(I_3)_{5/3}$	15.7	0.04	3.0

a) All Se or S parameters for the disordered Se.

As shown in Fig. 7(b), the thermoelectric power of (**1c**)$(I_3)_{5/3}$ and (**1d**)$(I_3)_{5/3}$ is negative. This is associated with the large charge transfer that exceeds half-filled. The HOMO band is 1/6-filled, and leads to electron-like conduction and negative thermoelectric power. The room-temperature values, $-53\ \mu V\ K^{-1}$ for (**1c**)$(I_3)_{5/3}$ and $-42\ \mu V\ K^{-1}$ for (**1d**)$(I_3)_{5/3}$, increase as the Se content increases (cf. $-56\ \mu V\ K^{-1}$ for (TTM-TTP)$(I_3)_{5/3}$). Assuming the one-dimensional tight-binding band, we can estimate the bandwidth to be 0.9 eV for (**1c**)$(I_3)_{5/3}$ and 1.1 eV for (**1d**)$(I_3)_{5/3}$ (cf. 0.9 eV for (TTM-TTP)$(I_3)_{5/3}$). These results mean that the selenium substitution enlarges the bandwidth. The temperature dependence is in agreement with the electrical resistivity measurements; the thermopower of (**1c**)$(I_3)_{5/3}$ gradually diverges below 100 K, whereas (**1d**)$(I_3)_{5/3}$ maintains metallic behavior down to 3 K. This temperature dependence is consistent with the constant temperature dependence of the resistivity of (**1d**)$(I_3)_{5/3}$.

Energy Band Structures of (1c)$(I_3)_{5/3}$ and (1d)$(I_3)_{5/3}$. The intermolecular overlap integrals calculated from HOMO, where a is along the stack, and b, and c are interstack ones, are listed in Table 6.[25,26] For (**1c**)$(I_3)_{5/3}$, we have carried out two calculations where the disordered selenium atoms are treated as selenium atoms and as sulfur atoms, respectively. When selenium parameters are used, the calculated a interaction, which directly determines the band width, increases by 30% in comparison with the value for the TTM-TTP compound. The thermoelectric power measurements, however, indicate that the bandwidth of (**1c**)$(I_3)_{5/3}$ is about the same as that of (TTM-TTP)$(I_3)_{5/3}$. On the other hand, the interstack interaction c of (**1d**)$(I_3)_{5/3}$ increases by about three times, and amounts to as much as 67% of the intrachain interaction. Since the expansion of the lattice constant *c* is small, the chalcogen–chalcogen distances between the neighboring terminal groups are almost the same: 4.12 Å for (TTM-TTP)$(I_3)_{5/3}$,[18] 4.13 Å for (**1c**)$(I_3)_{5/3}$, and 4.12 Å for (**1d**)$(I_3)_{5/3}$. Consequently, the Se–Se contacts give rise to the large interchain c interaction values. When selenium parameters are used in (**1c**)$(I_3)_{5/3}$, the c interaction is similarly enhanced, but is not very large for the calculation using the sulfur parameters.

The tight-binding energy band structure and the Fermi surface, calculated on the basis of the above overlap integrals, are depicted in Fig. 8 together with those of (TTM-TTP)$(I_3)_{5/3}$. For (**1c**)$(I_3)_{5/3}$, the results of the sulfur parameters are used, because this gives more reasonable bandwidth and c interaction values. The Fermi surface varies from one-dimensional in (TTM-TTP)$(I_3)_{5/3}$ to considerably two-dimensional in (**1d**)$(I_3)_{5/3}$, in which a small electron-like pocket is constructed. This change comes from an increase of the interstack interaction c. A one-dimensional system is more susceptible to electron correction than a two-dimensional system. This enhanced two-dimensionality explains the suppression of the M–I transition in (**1d**)$(I_3)_{5/3}$. The stabilization of the metallic phase is directly related to the selenium substitution.

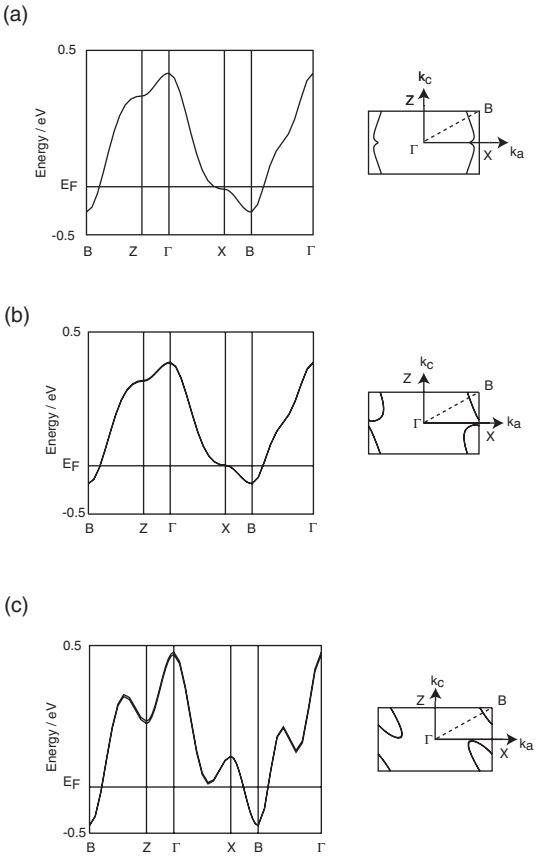

Fig. 8. Band structure and Fermi surface of the 5/3-phase salts. (a) (TTM-TTP)$(I_3)_{5/3}$, (b) (**1c**)$(I_3)_{5/3}$, and (c) (**1d**)$(I_3)_{5/3}$. The calculation of sulfur parameters for disordered Se atoms is used for (**1c**)$(I_3)_{5/3}$.

Summary

We have prepared selenium containing TTM-TTP derivatives, in which the 1,3-dithiole rings of the bis-fused TTF framework as well as the terminal methylthio groups have been substituted. In particular, it should be noted that TTM-DSDTP (**1a**) is the first example where the tetrathiapentalene (TTP) core is substituted.

Several charge-transfer salts of the present donors have been formed by electrochemical oxidation. The selenium substitution to the inner TTP part has given 1:1 salts, (**1a**)I_3 and (**1a**)$GaCl_4$. (**1a**)I_3 has a trimer structure and exhibits semiconductive behavior. (**1a**)$GaCl_4$ is isostructural to (TTM-TTP)-$FeBr_{1.8}Cl_{2.2}$, and the suppression of the steep increase of resistivity down to 60 K is attributable to the enhanced band width. This M–I transition temperature 60 K is one of the lowest values recorded among the 1:1 composition metallic salts. The selenium substitution in the outer rings has afforded the (TTM-TTP)$(I_3)_{5/3}$-type salts; although the M–I transition of the I_3 salt of **1c**, the asymmetrically Se-substituted donor, is not suppressed, probably owing to the positional selenium disorder, the M–I transition is entirely suppressed in the I_3 salt of the

symmetrically substituted **1d**. The calculation of overlap integrals (as well as band structure) shows that this is associated with the enhanced interchain interaction. These findings demonstrate that selenium substitution is a versatile way to stabilize the metallic phase in the TTP conductors. The preparation of other varieties of selenium containing TTP donors and charge-transfer salts are under investigation.

Experimental

General Data. Trimethyl and triethyl phosphites were purified under nitrogen by fractional distillation. The melting points were determined with a Yanaco MP micro melting point apparatus. NMR spectra were obtained with a JEOL JNM-AL300 spectrometer. MS spectra were obtained with a Shimadzu QP-5000 for EI-MS, and with a Shimadzu AXIMA-CFR for MALDI-TOF-MS. IR spectra were recorded on a SHIMADZU FTIR-8000 spectrometer. Cyclic voltammograms were measured on a Yanaco VMA-010 spectrometer.

Syntheses. 4,5-Bis[2-(methoxycarbonyl)ethylthio]-1,3-diselenol-2-one (3): To a solution of 4,5-bis[2-(methoxycarbonyl)-ethylthio]-1,3-diselenole-2-selone (0.32 g, 0.63 mmol) dissolved in chloroform–acetic acid (3/1 = v/v, 90 mL), mercury(II) acetate (0.75 g, 2.4 mmol) was added, and the resulting suspension was stirred at room temperature for 2 h. The resulting white solid was filtered off and washed with chloroform, and the combined filtrate was washed with water (50 mL × 2), aqueous potassium carbonate (50 mL × 2), and water again (50 mL × 1), and then dried over $MgSO_4$. Evaporation of the solvent gave a pale yellow solid (0.22 g, 77%). Mp 43 °C; IR (KBr) ν_{max} 1734 (s), 1692 (s), 1157 (m) cm^{-1}; ^1H NMR ($CDCl_3$, 300 MHz) δ 2.72 (t, 4H, J = 7.4 Hz), 3.14 (t, 4H, J = 7.4 Hz), 3.72 (s, 6H); MS m/z 450 (M^+).

2,3-Bis[2-(methoxycarbonyl)ethylthio]-6,7-bis(methylthio)-1,4-diselena-5,8-dithiafulvalene (5): 4,5-Bis(methylthio)-1,3-dithiole-2-thione **4** (0.33 g, 1.46 mmol) and 4,5-bis[2-(methoxycarbonyl)ethylthio]-1,3-diselenol-2-one **3** (0.21 g, 0.47 mmol) were heated in triethyl phosphite (7 mL) at 110 °C under nitrogen atmosphere for 2 h. After the triethyl phosphite was evaporated in vacuo, the residue was chromatographed on silica gel with CH_2Cl_2 as the eluent to afford **5** (0.27 g, 96%) as a red oil. IR (KBr) ν_{max} 2949 (w), 2345 (w), 1737 (s), 1435 (m), 1173 (m) cm^{-1}; ^1H NMR ($CDCl_3$, 300 MHz) δ 2.43 (s, 6H), 2.69 (t, 4H, J = 7.2 Hz), 3.09 (t, 4H, J = 7.2 Hz), 3.72 (s, 6H); MS m/z 628 (M^+).

5-[4,5-Bis(methylthio)-1,3-dithiol-2-ylidene]-1,3-dithia-4,6-diselenapentalen-2-one (6): Diselenadithiafulvalene **5** (0.33 g, 0.53 mmol) and CH_3ONa (0.36 g, 6.66 mmol) were reacted in acetone (2 mL) and methanol (1.5 mL) under nitrogen atmosphere for 40 min. Anhydrous zinc chloride (0.06 g, 0.44 mmol) in 1.0 mL methanol and tetrabutylammonium bromide (0.23 g, 0.71 mmol) in 1.0 mL methanol were successively added. The formed precipitates were collected by filtration, washed with methanol, and dried in vacuo. The residue was suspended in THF (5 mL), and cooled to −80 °C. Bis(trichloromethyl) carbonate (triphosgene, 0.12 g, 0.43 mmol) in THF (3.0 mL) was dropwise added to the suspension, and the resulting mixture was allowed to warm to room temperature. The solvent was removed by a rotary evaporator, and the residue was treated with methanol. The resulting precipitate was collected by filtration, washed with water and methanol, and dried in vacuo. The crude product **6** (0.12 g, 47%) was obtained as a pale yellow solid. No further purification was carried out, due to the low solubility of the compound **6**. Mp 206–208 °C (dec.); IR (KBr) ν_{max} 1649 (s) cm^{-1}; ^1H NMR ($CDCl_3/CS_2$ = 1/1, 300 MHz) δ 2.42 (s, 6H); MS (MALDI-TOF) m/z 480 (M^+).

2,5-Bis[4,5-bis(methylthio)-1,3-dithiol-2-ylidene]-1,3-diselena-4,6-dithiapentalene (TTM-DSDTP, 1a): Dithiadiselenapentalen-2-one **6** (0.06 g, 0.128 mmol) and 4,5-bis(methylthio)-1,3-dithiole-2-thione **4** (0.17 g, 0.75 mmol) were reacted in 3.0 mL trimethyl phosphite and 4.0 mL toluene at 110 °C under nitrogen atmosphere for 2 h. The reaction mixture was cooled, and the resulting precipitate was collected by filtration, washed with hexane and methanol, and dried in vacuo. Chromatography (silica gel, CS_2) afforded a brown solid of **1a** (31 mg, 38%). Mp 224–225 °C (dec.); IR (KBr) ν_{max} 2910 (w), 1425 (w), 1305 (w) cm^{-1}; ^1H NMR ($CDCl_3/CS_2$ = 1/1, 300 MHz) δ 2.43 (s, 12H); MS (MALDI-TOF) m/z 659 (M^+); Anal. Calcd for $C_{14}H_{12}S_{10}Se_2$: C, 25.52; H, 1.84; S, 48.67%. Found: C, 25.75; H, 1.97; S, 48.41%. Compounds **1b**–**1d** were prepared similarly.

2,5-Bis[4,5-bis(methylthio)-1,3-diselenol-2-ylidene]-1,3,4,6-tetrathiapentalene (TTM-BDS-TTP, 1b): 10% yield; brown solid; mp 260–261 °C (dec.); IR (KBr) ν_{max} 2911 (w), 2365 (w), 1420 (w) cm^{-1}; ^1H NMR ($CDCl_3/CS_2$ = 1/1, 300 MHz) δ 2.34 (s, 12H); MS (MALDI-TOF) m/z 753 (M^+). Reliable elemental analysis data were not obtained due to the insufficient sample amount.

2-[4,5-Bis(methylthio)-1,3-dithiol-2-ylidene]-5-[4,5-bis(methylseleno)-1,3-diselenol-2-ylidene]-1,3,4,6-tetrathiapentalene (DTM-DSM-TS-TTP, 1c): 20% yield; pale orange solid; mp 226–227 °C (dec.); IR (KBr) ν_{max} 2915 (w), 2345 (w), 1414 (w) cm^{-1}; ^1H NMR ($CDCl_3/CS_2$ = 1/1, 300 MHz) δ 2.33 (s, 6H), 2.40 (s, 6H); MS (MALDI-TOF) m/z 753 (M^+); Anal. Calcd for $C_{14}H_{12}S_8Se_4$: C, 22.34; H, 1.61; S, 34.08%. Found: C, 22.01; H, 1.72; S, 34.70%.

2,5-Bis[4,5-bis(methylseleno)-1,3-diselenol-2-ylidene]-1,3,4,6-tetrathiapentalene (TSM-BDS-TTP, 1d): 16% yield; brown solid; mp 253–254 °C (dec.); IR (KBr) ν_{max} 2910 (w), 2367 (w), 1411 (w) cm^{-1}; ^1H NMR ($CDCl_3/CS_2$ = 1/1, 300 MHz) δ 2.35 (s, 12H); MS (MALDI-TOF) m/z 941 (M^+); Anal. Calcd for $C_{14}H_{12}S_4Se_8$: C, 17.88; H, 1.29; S, 13.64%. Found: C, 18.26; H, 1.32; S, 13.85%.

Electrochemical Crystal Growth. Crystals were grown by electrochemical oxidation in the organic solvents indicated below in the presence of the donor (2 mg) and the tetrabuthylammonium salts (50 mg) of the corresponding anions under a constant current at room temperature using H-shaped cells with Pt electrodes for one week; Copper plates of (**1c**)$(I_3)_{5/3}$ and (**1d**)$(I_3)_{5/3}$, and black needles of (**1a**)I_3 were obtained in chlorobenzene under 1.0 μA current, whereas black blocks of (**1a**)$GaCl_4$ were obtained in 1,2-dichloroethane under 0.5 μA current.

X-ray Analysis. The crystal structures of the four compounds were determined from single-crystal X-ray diffraction. The data of (**1a**)$GaCl_4$, (**1c**)$(I_3)_{5/3}$, and (**1d**)$(I_3)_{5/3}$ were measured by ω scan technique on a Rigaku automated four-circle diffractometer AFC-7R with graphite monochromatized Mo Kα radiation ($2\theta < 60°$). In the case of (**1a**)I_3, measurements were made on a Quantum CCD area detector on a Rigaku AFC-7R X-ray diffractometer with graphite monochromatized Mo Kα radiation. The structures were solved by the direct method: SIR 97 for (**1a**)I_3 and (**1d**)$(I_3)_{5/3}$, and SIR 92 for (**1a**)$GaCl_4$ and (**1c**)$(I_3)_{5/3}$. The structures were refined by the full-matrix least-squares procedure by applying anisotropic temperature factors for all non-hydrogen atoms except for (**1d**)$(I_3)_{5/3}$, in which isotropic temperature factors were applied to several atoms on account of relatively poor crystal quality. Crystallographic data have been deposited at the CCDC, 12 Union Road, Cambridge CB2 1EZ, UK and copies can be

obtained on request, free of charge, by quoting the publication citation and the deposition numbers CCDC 225450–225453.

Transport Properties. Electric resistivity was measured for single crystals by the four-probe method using a low frequency ac current (usually 10 μA). Electrical contacts to the crystals were made with 15-μm gold wire and gold paint. The crystals were held in a cryostat, and the temperature was monitored by a Cu–Constantan thermocouple for temperatures above 50 K and a carbon resister sensor for temperatures below 50 K. Thermoelectric power measurements were carried out by making two-probe electrical contacts attached to two heat sinks with gold foil and gold paint.

We thank Dr. Hiroki Akutsu of the Department of Material Science, Himeji Institute of Technology, for measuring the X-ray reflection data with a Quantum CCD area detector on a Rigaku AFC-7R X-ray diffractometer. We are grateful for financial support from a Grant-in-Aid for Scientific Research on Priority Areas of Molecular Conductors (No. 15073211) from the Ministry of Education, Culture, Sports, Science and Technology.

References

1 F. Wudl, J. M. Smith, and E. J. Hufnagel, *J. Chem. Soc., Chem. Commun.*, **1970**, 1453.

2 T. Ishiguro, K. Yamaji, and G. Saito, "Organic Superconductors," 2nd ed, Springer-Verlag, Berlin, Heidelberg (1998); J. M. Williams, J. R. Ferraro, R. J. Thorn, K. D. Carlson, U. Geiser, H. H. Wang, A. M. Kini, and M.-H. Whangbo, "Organic Superconductors (Including Fullerenes)," Prentice Hall, New Jersey (1992).

3 L. B. Coleman, M. J. Cohen, D. J. Sandman, F. G. Yamagishi, A. F. Garito, and A. J. Heeger, *Solid State Commun.*, **12**, 1125 (1973); "Highly Conducting One-Dimensional Solids," ed by J. T. Devreese, R. P. Evrard, and V. E. van Doren, Plenum Press, New York (1979).

4 E. M. Engler and V. V. Patel, *J. Am. Chem. Soc.*, **96**, 7376 (1974).

5 K. Bechgaard, D. O. Cowan, and A. N. Bloch, *J. Chem. Soc., Chem. Commun.*, **1974**, 937; D. Jérome, A. Mazaud, and M. Ribault, *J. Phys. Lett.*, **41**, L95 (1980).

6 J. M. Williams, *Inorg. Synth.*, **24**, 130 (1987); V. Y. Lee, E. M. Engler, R. R. Schumaker, and S. S. P. Parkin, *J. Chem. Soc., Chem. Commun.*, **1983**, 235; A. Moradpour, V. Peyrussan, I. Johansen, and K. Bechgaard, *J. Org, Chem.*, **48**, 388 (1983); R. Kato, H. Kobayashi, and A. Kobayashi, *Synth. Met.*, **41–43**, 2093 (1991); J. Yamada, Y. Amano, S. Takasaki, R. Nakanishi, K. Matsumoto, S. Satoki, and H. Anzai, *J. Am. Chem. Soc.*, **117**, 1149 (1995).

7 F. Ogura and K. Takimiya, "Organoselenium Chemistry, A Practical Approach," ed by T. G. Back, Oxford University Press, New York (1999), p. 258.

8 K. Takimiya, A. Morikami, and T. Otsubo, *Synlett*, **1997**, 319.

9 K. Takimiya, Y. Kataoka, Y. Aso, T. Otsubo, H. Fukuoka, and S. Yamanaka, *Angew. Chem., Int. Ed.*, **40**, 1122 (2001); K. Takimiya, A. Takamori, Y. Aso, T. Otsubo, T. Kawamoto, and T. Mori, *Chem. Mater.*, **15**, 1225 (2003); K. Takimiya, T. Jigami, M. Kawashima, M. Kodani, Y. Aso, and T. Otsubo, *J. Org. Chem.*, **67**, 4218 (2002); K. Takimiya, Y. Kataoka, N. Niihara, Y. Aso, and T. Otsubo, *J. Org. Chem.*, **68**, 5217 (2003); M. Kodani, A. Takamori, K. Takimiya, Y. Aso, and T. Otsubo, *J. Solid State Chem.*, **168**, 582 (2002).

10 T. Mori, T. Kawamoto, Y. Misaki, K. Kawakami, H. Fujiwara, T. Yamabe, H. Mori, and S. Tanaka, *Mol. Cryst. Liq. Cryst.*, **284**, 271 (1996).

11 Y. Misaki, H. Nishikawa, K. Kawakami, S. Koyanagi, T. Yamabe, and M. Shiro, *Chem. Lett.*, **1992**, 2321.

12 T. Mori, H. Inokuchi, Y. Misaki, T. Yamabe, H. Mori, and S. Tanaka, *Bull. Chem. Soc. Jpn.*, **67**, 661 (1994).

13 T. Mori, T. Kawamoto, K. Iida, J. Yamaura, T. Enoki, Y. Misaki, T. Yamabe, H. Mori, and S. Tanaka, *Synth. Met.*, **103**, 1885 (1999).

14 M. Katsuhara, M. Aragaki, T. Mori, Y. Misaki, and K. Tanaka, *Chem. Mater.*, **12**, 3186 (2000).

15 M. Katsuhara, M. Aragaki, S. Kimura, T. Mori, Y. Misaki, and K. Tanaka, *J. Mater. Chem.*, **11**, 2125 (2001).

16 K. Takimiya, A. Ohnishi, Y. Aso, T. Otsubo, F. Ogura, K. Kawabata, K. Tanaka, and M. Mizutani, *Bull. Chem. Soc. Jpn.*, **67**, 766 (1994).

17 H. P. Choi, Y. Okano, H. Fujiwara, H. Kobayashi, and A. Kobayashi, to be published.

18 T. Mori, Y. Misaki, and T. Yamabe, *Bull. Chem. Soc. Jpn.*, **70**, 1809 (1997).

19 T. Mori, T. Kawamoto, Y. Misaki, and K. Tanaka, *Bull. Chem. Soc. Jpn.*, **71**, 1321 (1998).

20 Y. Misaki, T. Kochi, T. Yamabe, and T. Mori, *Adv. Mater.*, **10**, 588 (1998); Y. Misaki, M. Taniguchi, K. Tanaka, K. Takimiya, A. Morikami, T. Otsubo, and T. Mori, *Chem. Lett.*, **1999**, 859; T. Kaibuki, Y. Misaki, K. Tanaka, K. Takimiya, A. Morikami, and T. Otsubo, *Synth. Met.*, **102**, 1621 (1999); M. Taniguchi, Y. Misaki, K. Tanaka, T. Yamabe, and T. Mori, *Synth. Met.*, **102**, 1721 (1999); M. Taniguchi, Y. Misaki, T. Yamabe, K. Tanaka, K. Murata, and T. Mori, *Solid State Commun.*, **111**, 559 (1999); J. Yamada, S. Satoki, S. Mishima, N. Akashi, K. Takahashi, N. Masuda, Y. Nishimoto, S. Takasaki, and H. Anzai, *J. Org. Chem.*, **61**, 3987 (1996).

21 H. Fujiwara, Y. Misaki, T. Yamabe, T. Mori, H. Mori, and S. Tanaka, *J. Mater. Chem.*, **10**, 1565 (2000).

22 M. Kodani, K. Takimiya, Y. Aso, T. Otsubo, T. Nakayashiki, and Y. Misaki, *Synthesis*, **2001**, 1614; K. Takimiya, K. Yamane, Y. Aso, and T. Otsubo, *Mol. Cryst. Liq. Cryst.*, **379**, 65 (2002).

23 M. Ashizawa, H. Nii, T. Kawamoto, T. Mori, Y. Misaki, K. Tanaka, K. Takimiya, and T. Otsubo, *Synth. Met.*, **135–136**, 627 (2003); M. Ashizawa, H. Nii, T. Mori, Y. Misaki, K. Tanaka, K. Takimiya, and T. Otsubo, *Bull. Chem. Soc. Jpn.*, **76**, 2091 (2003).

24 Bond lengths of C=C bonds are C_3=C_4: 1.35(2), C_5=C_6: 1.35(2), C_7=C_8: 1.34(2), C_9=C_{10}: 1.34(2), C_{11}=C_{12}: 1.33(2) Å for the molecule A and C_{17}=C_{18}: 1.36(2), C_{19}=C_{20}: 1.36(2), C_{21}=C_{21}: 1.33(2) Å for the molecule B.

25 T. Mori, A. Kobayashi, Y. Sasaki, H. Kobayashi, G. Saito, and H. Inokuchi, *Bull. Chem. Soc. Jpn.*, **57**, 627 (1984).

26 T. Mori and M. Katsuhara, *J. Phys. Soc. Jpn.*, **71**, 826 (2002); T. Kawamoto, T. Mori, C. Terakura, T. Terashima, S. Uji, H. Tajima, K. Takimiya, Y. Aso, and T. Otsubo, *Eur. Phys. J. B*, **36**, 161 (2003).

27 If the disordered selenium atoms are treated as sulfur atoms, the calculated overlap integrals are b: −0.20, p1: 0.15, p2: 0.13, p3: 0.02×10^{-3}.

28 P. Coppens, "Extended Linear Chain Compounds I," ed by J. S. Miller, Plenum, New York (1982), p. 333.